IJAF - Instrumentcenter for Jordbaseret Astronomisk Forskning
Astronomisk Observatorium, Juliane Maries Vej 30, DK-2100 København Ø, Danmark.

Astronomical Instrument Centre

Report # 2: Image quality at the Nordic Optical Telescope

by

Michael I. Andersen & Anton Norup Sørensen
Copenhagen University Observatory

February 29. - 1996

Abstract

The image quality of the Nordic Optical Telescope is investigated by comparing image quality measurements from CCD data with simultaneous seeing data obtained with the nearby IAC seeing monitor. We find a difference between the seeing monitor and the image quality at the NOT of $0\farcs25 \pm 0\farcs05$. We attempt to estimate the sources of aberration, and show that they may account for the difference. We conclude, that if the image quality of the telescope is optimized, a median image quality of $\approx 0\farcs4$ should be obtainable during the summer season, using tip/tilt correction.

Contents

1 Introduction

Among Nordic astronomers, the Nordic Optical Telescope is known as being one of the best telescopes in the world for direct imaging. This reputation have left the community with the impression that little can be done to improve the image quality at the NOT. The aim of this report is to show that this is in fact not true, and that significant improvements can be achieved. We will also show, that the realization of these improvements, in combination with tip/tilt correction, will result in an image quality beyond the present state of the art at astronomical observatories.

2 Factors degrading the image quality of a telescope

At observing sites of excellent quality, other factors than atmospheric seeing may influence the angular resolution, even if great care is taken to construct a high quality observatory. We summarize the sources of aberration that may degrade image quality at an observatory. Later, these are treated in detail in the context of the NOT.

- Dome and mirror seeing.

  Temperature differences between the ambient air and the telescope and internal dome structure will lead to convective heat transport, inducing a non homogeneous and time dependent structure in the refractive index of the air.

  While the temperature of dome and telescope structure settles relatively fast in a well ventilated dome, the large thermal inertia of a primary mirror may cause a significant temperature gradient in the air just above the mirror. This leads to convective motion, producing what is usually labeled *mirror seeing*.

  At the CFHT, an excess seeing of $0\overset{''}{.}40 \cdot \Delta T_{mirror}^{6/5}$ was found when the mirror was warmer than ambient air, while no significant degradation was seen for a slightly undercooled mirror [Racine 91]. The excess seeing was ascribed to mirror seeing. This interpretation is however questionable, because the mirror temperature is in general a tracer of the thermal imbalance in the dome and building as a whole.

- Thermal effects

  These effects appear as a static aberration along the edge of the pupil. They arise as a result of a boundary layer due to a different temperature/thermal balance of mechanical parts (typically sky baffles, mirror cover, tube center piece etc.) close to the light path.

- Low order telescope aberrations.

  Abberations are introduced by improper collimation of the telescope and by large scale deformations of the mirrors. These aberrations typically depend on telescope altitude due to the changing gravitational stress, i.e. they arise because of improper mechanical support.

  The typical effect of these aberrations in case of small amplitudes is a broadening of the core of the point spread function.

- Mirror figuring errors.

  The surfaces of the mirrors have departures from the desired shape on all spatial scales, caused by deformation by mechanical forces, errors during polishing, scratches etc.

  Errors at scales smaller than what the mirror support can correct, can be labeled as figuring errors, ranging in size from the wavelength of light to typically a few tens of centimeters.

  Typically, figuring errors take flux from the core of the PSF and scatter this into the wings of the PSF.

- Focus.

  While telescope focus strictly speaking is a low order aberration, it is usually controlled by the observer. As focus change due to changes in the temperature of the telescope structure and attitude, the observer may have to correct the focus rather frequently to minimize focus errors. A quick and precise method for finding the focus may also be lacking.

- Post telescope aberrations.

  Any optical element introduce optical aberrations. This is also the case of filters and camera windows, although the proximity to focus of these elements significantly reduces the demands on these optical elements.

- Telescope oscillations.

  Deviations from perfect telescope tracking may occur on a wide range of time scales, some of which are too short for an auto guider to correct for. Mechanical oscillations may occur at frequencies of several Hertz, resulting in elongated images of point sources.

- Auto guider.

  While the task of the auto guider is to reduce tracking errors and in this way improve image quality, an improper implementation may reduce the gain.

  Oscillations may be induced by a too aggressive correction. As the reference star for auto guiding is placed several arcminutes away from the observed field, atmospheric image motion in the two fields may be uncorrelated. Perfect guiding on the reference star will then lead to increased image motion in the observed field.

3 Seeing on La Palma

Ambitious seeing monitoring programs on Rocque de Los Muchachos have been initiated by IAC as well as ING. These programs use the Differential Image Motion Monitor (DIMM) technique developed by ESO [Sarazin, M. 89]. The IAC DIMM is described by [Vernin, J. 95]. DIMM's basically measure the corrugation of the wavefront on scales of ≈20cm. The seeing is derived from this measure, assuming Kolmogorov turbulence with infinite outer scale

$$\Phi(k) \propto k^{-11/3} \tag{1}$$

3.1 The outer scale length and DIMM measurements

Within the last few years, it have become evident that the assumption of an infinite outer scale length L_0 is not valid. The turbulent layers in the atmosphere are ≈10m thick. Since structures larger than the thickness of the layer are unlikely to exist, the thickness is an upper limit for L_0. The normalization of DIMM measurements is therefore estimating a too large seeing.
At the NOT, we typically measure only 40-50% of the image motion predicted by Kolmogorov turbulence with infinite L_0. This is in accordance with the implication from the layered structure of the turbulence, that L_0 should be finite. When L_0 is finite, long slopes in the wavefront will be reduced. The average slope of the wavefront over a large telescope aperture is therefore smaller than with an infinite L_0. Accordingly, image motion is reduced. Under favorable wind conditions the ESO NTT can reach an image quality which is better than what is measured by the nearby La Silla DIMM. This is in support of the conclusion, that the DIMM is overestimating the seeing.

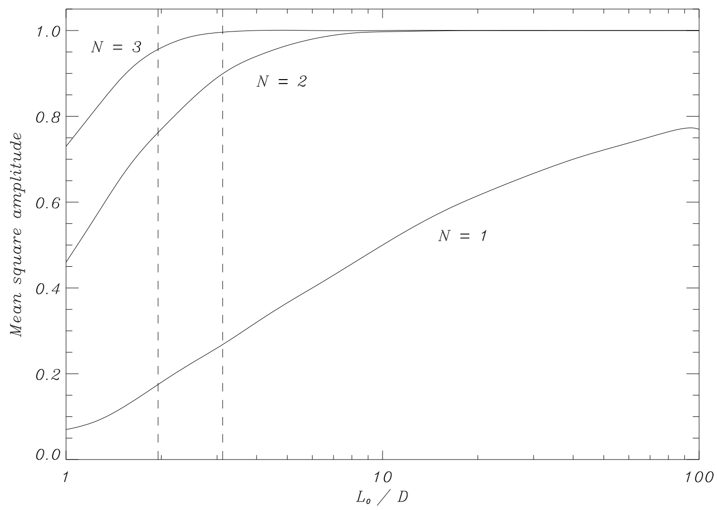

Figure 1: The mean square amplitude (the variance) of atmospheric aberration terms of radial order 1, 2 and 3 as function of the outer scale length L_0 in units of telescope diameters, normalized to the amplitude at infinite L_0. The range of L_0 = 5-8m in the case of the NOT is indicated with vertical dashed lines.

Recently, [Voitsekhovich, V. 95] calculated the lowest order Zernike aberration terms in the case of a finite L_0 (fig. 1). From these calculations we can directly estimate L_0 for the atmosphere above La Palma, by comparing the image motion predicted for an infinite L_0 to the measured image motion. We derive an L_0 of 5-8m, in excellent agreement with the limit set by the thickness of the turbulent layers. Unfortunately, the introduction of L_0 significantly complicates the theory of atmospheric turbulence and adaptive optics performance. The most immediate consequence is, that seeing, understood as the FWHM of the free atmosphere PSF, becomes a function of telescope diameter. Fig. 1 do also tell us, that the amplitude of higher order aberrations is essentially unaffected by a finite L_0 in the case of the NOT. From this we may draw two conclusions.

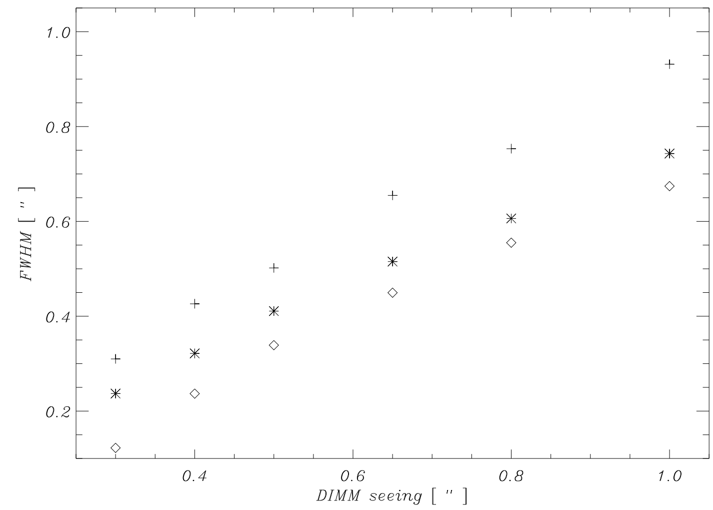

Figure 2: Correction of DIMM measurements in the case of an outer scale length of 8m. Shown is DIMM seeing (plus), L_0 corrected DIMM seeing (asterisk) and tip/tilt corrected DIMM seeing (diamonds).

- The error in the DIMM normalization is due to reduced image motion only.
- We can use the simpler $L_0 = \infty$ theory, when predicting the performance of higher order adaptive optics systems.

A correction, shown in fig. 2, of the DIMM measurements for $L_0 = 8$m has been obtained from simulations of atmospheric wavefronts with reduced tip/tilt.
C. Muñoz kindly made available for us IAC DIMM data from June 95. The IAC DIMM is placed close to the NOT, suggesting that the measurements should be a good indicator for the conditions at the NOT. For June as a whole, the median DIMM seeing is $0''.46$, with values ranging from $0''.22$ to above $1''$. By correction for L_0, we end up at a median seeing of $\approx 0''.38$ for June 1995.

4 Measured image quality vs. seeing

For the nights of the 27th and 28th of June 1995, we have simultaneous IAC DIMM data and NOT image quality data obtained by one of us (MIA) using BroCamI. We are therefore in a position, which allows us to asses the optical performance of the NOT. The image quality was estimated using the BIAS data acquisition program for BroCamI. This is done by a least squares fit of a Gaussian to the PSF, giving the corresponding FWHM as the output. We have tested BIAS against synthetic Gaussians, and the result typically agrees within $0''.02$ of the input FWHM.
A close eye was kept on the focus. The then just upgraded version of BIAS has a feature for plotting contour plots. This is a very neat tool for checking the focus. If the focus was off

by more than one (old) encoder unit, corresponding to a temperature change of $\approx$0.12 ^oC, the PSF began to show a signature of coma. Accordingly, focus had to be adjusted every 5-10 min. Obvious changes in the PSF during the observing run were noted in this way.

4.1 Correction of DIMM data

The DIMM data we received are reduced to the zenith at 500nm. It is not possible to reduce the image quality data to the same condition, since these data are affected by each of the aberration terms listed in section 2. Instead, we correct the DIMM data, such that they will be directly comparable to the image quality data. We use the following procedure:

- First the DIMM measurement is renormalized, using the result shown in fig. 2.
- Then the DIMM measurement is transferred to the zenith distance of the CCD observation by the well established relation

$$DIMM_z = DIMM_0 \times \sec(z)^{0.6} \tag{2}$$

- We then have to take into account the diffraction in the telescope, because the DIMM measurement is in principle for an infinitely large telescope. We do this by adding a constant term in a power of (5/3)

$$DIMM_d = (DIMM_z^{5/3} + 0.0996^{5/3})^{3/5} \tag{3}$$

  We find the constant term from the 80% encircled energy diameter of the perfect PSF at 500nm, reducing it by a factor 1.31, which is the ratio between the 80% encircled energy diameter and the FWHM of a Gaussian.

- As the last step, the DIMM measurement is transferred to the wavelength of observation

$$DIMM_{corrected} = (DIMM_d * (\lambda/500)^{-0.2} \tag{4}$$

Except for the renormalization of the DIMM measurement, the corrections we apply are on average small, of the order of or less than 0.″02.

4.2 Comparison of corrected DIMM data and image quality

The final data sample consists of 65 pairs of simultaneous DIMM and CCD measurements. The exposure time is ranging from 20 sec. to 20 min. DIMM measurements are made every 30 sec, with some interruptions. For short CCD exposures we have taken an average of the DIMM measurements over a 4 min. period around the exposure. We plot the corrected DIMM measurements vs. the NOT image quality in fig. 3. There is not a clear correlation between the DIMM measurement and the image quality. The RMS scatter of the difference between image quality and DIMM measurement is 0.″11. From the time evolution of the DIMM measurements, we estimate that at most 0.″05 is due to statistical fluctuations in this measurement. The DIMM and the NOT are separated by a few hundred meters, which may introduce some scatter. If the

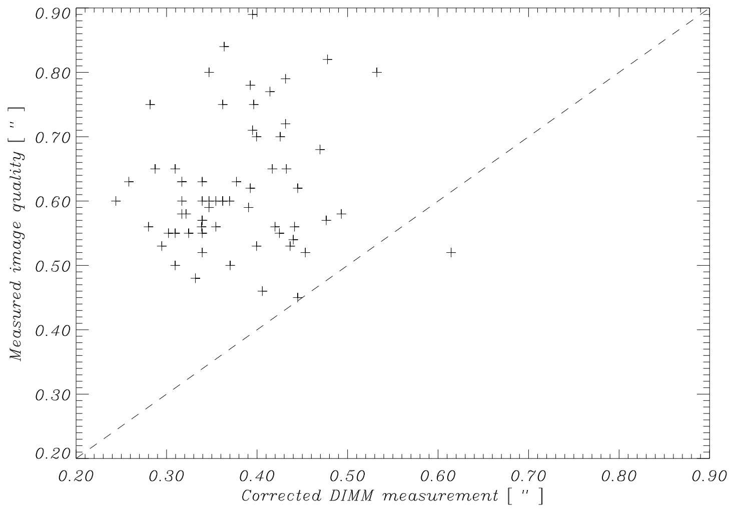

Figure 3: The measured image quality vs. corrected DIMM measurement for the complete data sample.

wind direction is north east, the air passing the DIMM first has to pass Cruz del Fraile, (the ridge where the NOT is located) lifting off the boundary layer. Fig. 5 indicate, that a major contribution to the scatter is dome seeing. Most of the aberration terms in the telescope are not stable and will also contribute to the scatter. The seeing measurements cover a narrow range only, and this may explain the apparent lack of a correlation. The fact, that we occasionally obtain an image quality which is better than the DIMM, show that the DIMM measurement do not have a significant bias towards smaller seeing values.

Histograms of the image quality and DIMM measurements are shown in fig. 4. The median value of the measured image quality is $0\farcs60$, and the median value of the corrected DIMM measurements is $0\farcs36$, yielding a typical difference of $0\farcs24$.

The median value of the reduced but uncorrected DIMM measurements used in this analysis is $0\farcs45$, and therefore essentially identical to the median of the month as a whole. We may therefore claim, that seeing conditions during the observations used in this analysis are typical summer season conditions (or at least typical for June 1995). The median image quality of $0\farcs60$ is however some what better than what is typically reported. Harri Lindgreen claim, that the most frequently encountered image quality during summer season is close to $0\farcs65$. In section 6 we show that at least part of this difference may be due to a less precise focusing by the average observer, which may be considered a simple consequence of lacking tools for analyzing focus exposures.

We therefore find ourselves in a situation, where we are ready to put forward the outrageous claim, that the difference in image quality of a *perfect NOT* and the *present NOT* is $0\farcs65 - 0\farcs36 = 0\farcs29$. Given the number of steps we went through before ending up at this result, we find it more reasonable to give the result in round numbers, by stating that the average image quality degradation at the NOT is $0\farcs25 \pm 0\farcs05$.

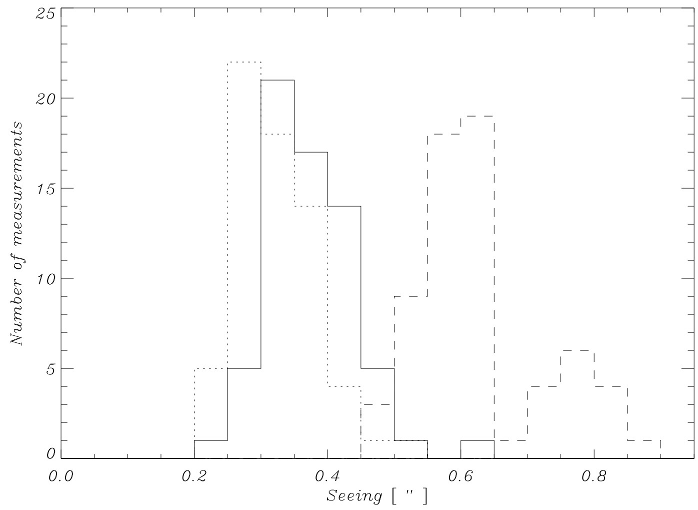

Figure 4: Histogram of measured image quality (dashed line), corrected DIMM data (full line) and fully tip/tilt corrected DIMM data.

5 The importance of the individual aberration terms

In this section we will try to estimate the contribution of the different aberration terms. We do this for a wavelength of 500nm. We will adopt a seeing of 0.″39, which corresponds to the median value of the sample of corrected DIMM data at this wavelength. For some of the sources of aberration we have some knowledge of their amplitude, for others we have little or no evidence, and our estimates should therefore be considered with significant reservation. We want to stress that most of the terms are highly variable in time. It is common practice [Racine 91] to add aberration terms in a power of 5/3. For aberration terms, we adopt this

$$\omega_{abb}^{5/3} = \omega_{seeing}^{5/3} + \omega_{dome}^{5/3} + \omega_{thermal}^{5/3} + \omega_{figure}^{5/3} + \omega_{support}^{5/3} + \omega_{focus}^{5/3} + \omega_{optics}^{5/3} \tag{5}$$

It is our experience, that image motion is better described by adding the individual terms in a power of 2, such that the final image quality is described by

$$\omega^2 = \omega_{abb}^2 + \omega_{guiding}^2 + \omega_{oscillation}^2 \tag{6}$$

5.1 Dome and mirror seeing

Immediately after opening the dome and mirror cover at the beginning of an observing night, turbulent cells moving slowly across the mirror are easily visible by watching a strongly defocused bright star on the auto guider monitor. While atmospheric seeing is visible as a fixed pattern moving at uniform speed across the pupil, dome/mirror seeing appears as slow vortex like movements at localized parts of the light path. Using an air blower, we identified this phenomenon to be due to mixing of (hot?) air in the tube with ambient air entering through the opening between the mirror and the center piece of the telescope tube.

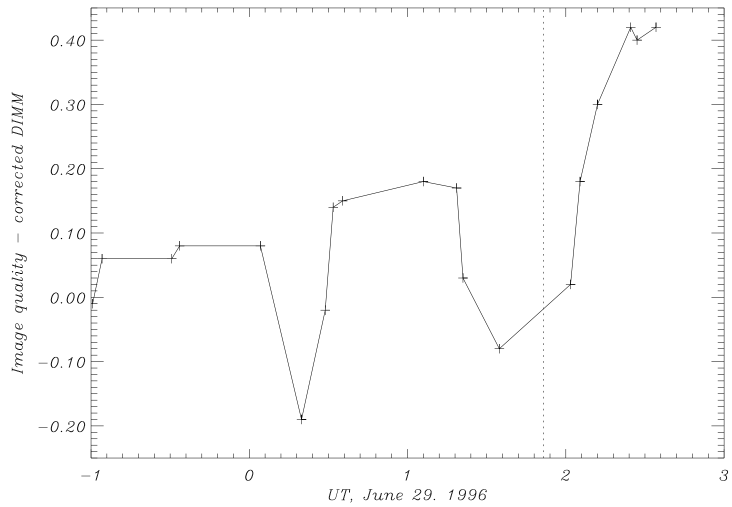

Figure 5: Difference between measured image quality and corrected DIMM measurement, as a function of time. The vertical dashed line indicate the moment when the telescope was turned from an up wind position to a down wind position.

During the June observing run, a repetitive behavior was noticed on four nights. During these nights, the wind was coming from the north and the mirror was typically 1-2^oC hotter than ambient air. At the beginning of the night, an object to the north was observed, facilitating a proper ventilation of the telescope. Past midnight, the telescope was pointed to an object opposite to the wind. During the next 10 minutes, the best images of the night were usually acquired. Following this, the image quality degraded by $0\farcs15$ - $0\farcs30$ through the next half hour, apparently depending on the wind speed. The interpretation of this as a dome seeing effect is supported by the difference between DIMM seeing and image quality, as shown in fig. 5. These observations indicate, that dome seeing effects may range from essentially zero to $0\farcs50$ or more. Here we shall adopt $\omega_{dome} = 0\farcs20$.

5.2 Thermal effects

We have no measurements or indications of thermal effects at the NOT. On La Silla it is common practice to remove Shack-Hartmann data points which are *too close* to the rim of the mirror, due to what is labeled as thermal effects. This suggest that such effects may also be present at the NOT. We will neglect it in this analysis, because we have no measurements.

5.3 Mirror figuring errors

As described by [Roddier, C. 93], the shape of the wavefront after passage of the optics of a telescope may be reconstructed from a pair of oppositly defocused long exposure images of a bright star. This method has been used at the NOT, giving maps of the optics with a resolution of 3.3 cm projected onto the primary mirror, approximately four times higher resolution than previous maps obtained. Two maps were produced, one showing aberration of higher order than defocus, and one showing the residual aberration after subtracting the 23 lowest Zernike polynomia, i.e. a slightly higher correction than is possible with the present active optics system at the NOT, leaving only figuring errors in the map.

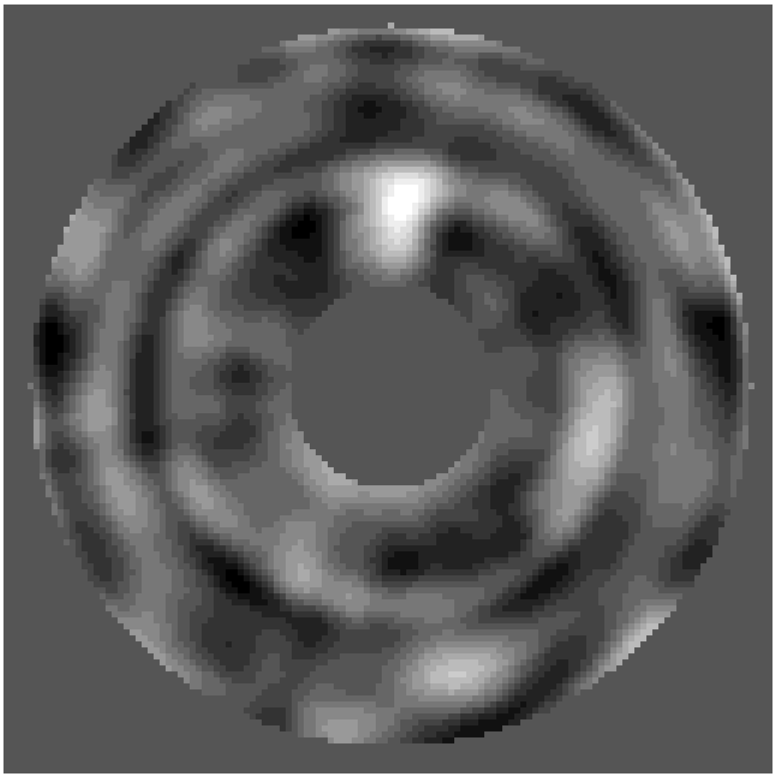

Figure 6: Residual aberration of the wavefront after subtraction of the 23 lowest Zernike terms. Six one-minute exposures were used for recording the map. The strongest local deviations in the map are about 200nm from the average.

With the low order aberrations subtracted, a map showing large scale details consistent with the map found by [Korhonen 92] is found. In addition, figuring errors on smaller scale is found, as can be seen on fig. 6 , most pronounced is a pattern of concentric rings.
The impact of figuring errors is best evaluated by generating a point spread function from the maps. In fig. 7, PSFs at 500nm are shown for a telescope without any aberrations, with all of the aberrations mapped by the defocus method and with the the aberrations attributed to figuring errors only.
The low order map results in a PSF with no core and a Strehl ratio of 0.09, i.e. a peak intensity of 9% of the peak intensity of the diffraction limited PSF. The 80% encircled energy diameter is $0''.58$. With the 23 lowest Zernike terms subtracted, the PSF has a core with a Strehl ratio of 0.74, and the 80% encircled energy diameter is $0''.38$.
In order to estimate the impact of mirror aberrations on image quality, we must examine the PSF from the combined aberrations from mirror and atmosphere. We generate a large number of instantaneous atmospheric wavefronts from a modified Komolgorov theory, taking into account the reduced image motion at NOT. The wavefronts are added to the mirror maps, and an average PSF is generated from the total set. Using the mirror map with the 23 first Zernike

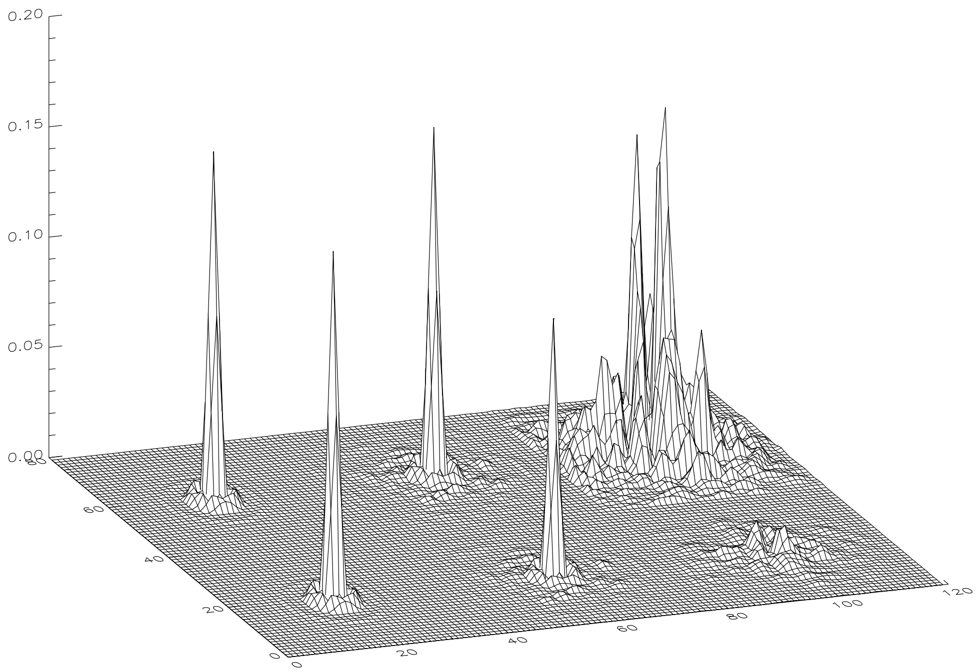

Figure 7: Point spread functions at a wavelength of 500nm, calculated from the phase-screens found from defocused images. Each PSF is shown in an array of 0″.75 size. *Front row, from left to right:* Un-aberrated PSF, PSF from map with 23 Zernike terms subtracted, PSF from complete map. Figures are normalized to the same total flux. *Back row:* Same PSF's, but normalized to same maximum local intensity.

terms subtracted, we find that $\omega_{figure} = 0''.10$.

5.4 Low order telescope aberrations

The thin mirror of the NOT is designed to be supported by the 45 bellows of the active optics system. Besides the benefit of a lower thermal inertia, this gives a great potential of compensating for deformations from gravitational stress and large scale mirror figuring errors. As the implementation of active optics still awaits completion, significant low order aberrations are often present. The 80% geometric encircled energy diameter measured using the wavefront sensor installed in the adaptor typically is 0″.3 to 0″.4 [Korhonen 92], depending on the zenith distance. Simulated corrections by [Korhonen 92] indicates that the 80% geometric encircled energy diameter would be reduced to 0″.2 with working active optics. The observer may often find these low order aberrations easily detectable, as astigmatism and coma are visible in slightly defocused images.

We estimate the contribution from low order aberrations following the procedure used to estimate ω_{figure}, but now adding all aberration terms. We find that $\omega_{support} = 0''.22$ for this specific measurement of the low order aberrations.

5.5 Focus

Focusing the NOT is giving rise to substantial frustration among observers. This is in part due to the high gamma factor of the telescope, which translates a small shift of the secondary with respect to the primary into a thirty times larger focus shift. As a further complication, no good tool to assist the observer is present. According to staff, there are big differences between observers in the effort put into focusing. We estimate that the typical focusing error corresponds to 4 (old) focus steps, which is equivalent to a temperature drift of 0.5 $^{\circ}C$. Again, using simulated atmospheric wavefronts, but adding a defocus corresponding to 4 steps, we find $\omega_{focus} = 0\farcs20$

5.6 Instrument optics

Typical filters are $\lambda/4$ per inch. With BroCamI, the filter is placed ≈100 mm from the CCD, where the convergent beam is ≈1/3 inch. From this we estimate a typical RMS wavefront error of $\lambda/30$, suggesting that $\omega_{optics} = 0\farcs03$. Most likely, significant differences between filters exist. The window is so close to the focus, that it can be ignored.

5.7 Telescope oscillations

At several occasions, we have observed telescope oscillations. The amplitude is dependent upon the wind speed. As a typical value, we find $\omega_{oscillation} = 0\farcs12$.

5.8 Auto guider

The auto guider at NOT consists of an intensified CCD camera producing a video signal, digitized by a frame grabber 25 times per second. At a rate of approx. 10 times per second, the centroid of a selected section of the frame is calculated, and the distance of the centroid from the center of the section is used as error signal to the auto guider. After a treatment which may consist of a low pass filtering, the error signal is fed to the servos.

On several occasions, the guide star has been observed to oscillate in position at a low frequency, visible on the auto guider monitor. Frequency analysis of motion of the guide star with and without auto guider has shown, that the auto guider corrects tracking errors below 0.1Hz and slightly amplifies image motion from 0.3 to 1Hz. Often a strong oscillation is started at approx. 0.3Hz, in some cases resulting in more overall image motion than when the telescope is blind tracking. Images appear elongated by several tenths of an arcsecond in these situations.

During *HiRAC* commissioning, we measured a very large isoplanatic patch, while auto guiding. This suggest that a significant part of the image motion we measure is due to tracking errors. It is very difficult to separate the different components of image motion. Here we will adopt $\omega_{guiding} = 0\farcs15$, again keeping in mind that this will change with conditions.

5.9 Image quality error budget

All error terms may now be added. In table 1, we list the estimated aberration contributions and resulting image quality. For each term, we also give the resulting image quality in their absence.

Table 1: Image quality error budget for the NOT.

Abberation term	Estimated contribution	Image quality if term absent
ω_{seeing}	0.39	0.47
ω_{dome}	0.20	0.59
$\omega_{thermal}$	0.00	0.66
ω_{figure}	0.10	0.63
$\omega_{support}$	0.22	0.58
ω_{focus}	0.20	0.59
ω_{optics}	0.03	0.66
$\omega_{guiding}$	0.15	0.63
$\omega_{oscillation}$	0.12	0.64
ω_{total}	0.65	

We do of course get the result we wanted. A median image quality of $0''.65$ is close to the typical good season seeing. According to table 1, the limiting image quality of the NOT, in the absence of seeing, is $0''.47$. This is apparently contradicted by the fact, that images of $0''.33$ have been acquired. According to C. Muñoz, the best seeing measured with the IAC DIMM is below $0''.20$, which corrected for a finite L_0 corresponds to a true seeing of $0''.14$. Dome seeing, low order aberrations and focus errors are however highly variable terms. If we reduce these terms by a factor of two relative to the values given in table 1, and assume the best seeing, we end up at an image quality of $0''.33$, while complete elimination of dome seeing and focus error will result in an image quality of $0''.27$.

6 Measures to improve the image quality at the NOT

In the light of the significant degradation of the image quality, it is appropriate to consider measures to improve it. We will not go into a detailed discussion, but try to give a list of the actions we could think off. These can basically be divided into two categories

- Diagnostic measures, which aims at a better understanding of the telescope and its environment.
- Actual improvements to the telescope and its environment.

We feel that diagnostic measures may be as important as actual improvements. For decades, the discussion of image quality at most observatories have been based on pure guess work. The fact, that image formation is a well understood physical process, should allow us to do this on a rational basis.

6.1 Minimizing the individual aberration terms

- Dome and mirror seeing

  We have suggested that $\omega_{dome} = 0\farcs20$ as a typical value, but have no hard evidence, only an indication that down wind observing seems to degrade the image quality. We have however more or less been forced to assume some dome seeing, otherwise it is difficult to account for the difference in image quality and DIMM seeing. We propose that *in situ* micro thermal sensors should be permanently installed at strategic points. They will allow us to measure local turbulence in real time. It should be possible to install a set of $\approx$10 sensors, including control system, for the equivalent of 2 months of cooling budget (50000USD). Such a system would also allow us to study how reduced cooling influences dome seeing, and thereby maybe help us saving a lot of money in the end.

  It seems obvious to consider improved mirror cooling. Forced ventilation of the mirrors and baffles during observation might reduce mirror seeing drastically. If the interpretation of fig. 5, that the degrading image quality is in fact due to dome seeing, we can also conclude, that the build up of dome seeing has a surprisingly long time constant of 10-20 mins. A ventilation system of moderate size should thus be able to cure the problem. Heat sources on the telescope and the instrument should be eliminated where possible.

- Thermal effects

  We do not know if we have such problems. An analysis could be done using the Korhonen-Hartmann wavefront sensor which we plan for ALFOSC. If thermal effects are identified, a careful redesign of baffles and mirror cover could be a solution.

- Mirror figuring errors

  An improved estimate of these should be made.

- Low order telescope aberrations

  This is one of the big problems. Active optics should obviously be made operational. The big question is in which way it should be operational. Are adjustments of the active optics once a night sufficient, or should it be done continuously as on the ESO NTT? Our experience with the telescope is, that aberrations change with time and not only altitude. This indicate, that a closed loop active optics system is required, if we should be able to utilize the best nights. This is a major undertaking. It could be implemented by replacing the guide probe with a Shack-Hartmann WFS, and then also use the WFS signal for guiding. Using an off axis WFS require a very good definition of the optical axis, and a care full calibration of the off axis astigmatism present in the Ritchey-Chretien telescope optics. We suggest that a study of the stability of the aberration terms is made, either with the present WFS or with the WFS to be implemented in ALFOSC.

  The performance of the support system is another critical issue. T. Korhonen (private communication) have indicated, that sticktion may be present in the radial supports.

- Focus

  This is another big problem. To keep a good focus, you really need to know the telescope. H. Schwartz suggest, that a closed loop system, utilizing interferometric measurement of the mirror distance is implemented. We strongly support this. We have considered to use the *HiRAC* guide probe as an auto focus unit, but have not implemented this. A closed loop WFS system would completely solve the focus drift problem, since the focus term would be measured optically on a continuous basis. We consider this one of the great virtues of a closed loop WFS.

As a starting point, tools for evaluation of a focus exposure should be made available.

- Instrument optics

  The optical quality of all filters should be checked. We should specify a high quality for filters to be used for high resolution imaging. The optical quality of instruments should be known.

- Telescope oscillations

  These have been a subject of discussion as long as the telescope has existed. I. Svaerd has demonstrated, that oscillations in the mirror can be induced by making a small jump in the control room. This indicates, that the problem will be difficult to solve. The essentially undamped pneumatic mirror support system may likely be at the core of the problem, and a replacement with a different kind of support may be the only solution. The oscillations severely compromise the performance to the tip/tilt system in *HiRAC*. At moderate to high wind speeds, even the passive image quality is affected.

- Auto guider

  In principle an auto guider is only required, if the telescope has problems with blind tracking. Our isoplanatic patch measurements during *HiRAC* commissioning show, that the auto guider is incapable of removing all tracking errors. Further observations are made, with the telescope in 'idle' mode. The tracking performance and auto guider performance should be analyzed in a common context. The solution to the problem could be an upgrade the alt-az encoders.

6.2 Goals for improvement of image quality

In the presence of the large number of error sources, we cannot expect a telescope to perform to the limit, even if we started from scratch. But it is instructive to se what could be obtained by setting realistic goals. In the following, we assume a four phases plan for improvement of image quality, each with an increasing demand on financial and labour resources.

- Phase 1: Improved focusing. Implement software for the analysis of focus exposures. Automatically correct focus as temperature and altitude change. Filter offsets.

- Phase 2: Tip/tilt correction fully implemented, problem with telescope oscillations still not solved, but auto guider errors reduced. Low order aberrations reduced by 1/3 through regular (weekly or so) use of WFS.

Table 2: Possible improvements to the image quality at the NOT.

Abberation term	Present state	Phase 1	Phase 2	Phase 3	Phase 4
ω_{seeing}	0.39	0.39	0.35	0.35	0.33
ω_{dome}	0.20	0.20	0.20	0.10	0.05
$\omega_{thermal}$	0.00	0.00	0.00	0.00	0.00
ω_{figure}	0.10	0.10	0.10	0.10	0.10
$\omega_{support}$	0.22	0.22	0.15	0.11	0.05
ω_{focus}	0.20	0.10	0.10	0.07	0.04
ω_{optics}	0.03	0.03	0.03	0.02	0.02
$\omega_{guiding}$	0.15	0.15	0.05	0.05	0.03
$\omega_{oscillation}$	0.12	0.12	0.12	0.12	0.03
ω_{total}	0.65	0.61	0.53	0.45	0.38

- Phase 3: Abberations reduced by a 50% through use of altitude dependent adjustment of active optics. Dome seeing reduced by 50% through improved mirror cooling and ventilation during observation. Auto focus. Use of high quality filters.

- Phase 4: Closed loop operation of WFS, aberrations reduced by 80%, focusing improved. We have understood most dome seeing effects by use of micro thermal sensors, and dome seeing is therefore reduced by 75%. Telescope oscillations reduced, tracking improved.

In table 2, we assume a set of improved aberrations terms resulting from each phase of upgrading. We adopt the median DIMM seeing of $0\farcs46$ (June 1995) and calculate the expected image quality on the basis of this.

7 Conclusion

By comparing IAC seeing monitor data with image quality data obtained with a direct CCD during normal observation, we have shown that the telescope significantly degrades the image quality.

From image motion data, we have been able to estimate the outer scale length of turbulence above La Palma to 5-8m, implying a much reduced image motion. Accordingly, the seeing monitor data are overestimating the true atmospheric seeing. By applying the appropriate correction, we conclude that the median summer season seeing on Rocque de Los Muchachos is $0\farcs39$, with the natural reservation, that small errors in the absolute normalization of DIMM measurements may exsist. This is to be compared to the typically image quality obtained at the NOT, which is $\approx 0\farcs65$ during the summer season.

An attempt is made to estimate the amplitude of each of the sources of aberration. Measurements of the optical aberrations in the telescope are available, which allow us to asses their relative importance. Dome seeing is a largely unknown factor, but our data gives evidence that dome seeing is at least occasionally the dominating factor. We also find that telescope motion, in the form of oscillations and guiding/tracking errors, is responsible for a significant fraction of the image motion observed at the NOT.

The key areas, where significant gains in image quality can be obtained, are active optics, improved ease of focusing and dome seeing. If the telescope is fully optimized, a tip/tilt corrected median seeing of $0\farcs40$ should be achievable. Occasionally, images below $0\farcs25$ should be obtainable.

References

[Korhonen 92] Korhonen, T. og Lappalainen, T. : **Interferometric Wavefront Sensor**, Progress in telescope and instrumentation technologies, Proc., ESO, April 1992, Editor Ulrich, M.

[Racine 91] Racine, R. et al. : **Mirror, Dome and Natural Seeing at CFHT**, PASP 103:1020-1032, September 1991

[Roddier, C. 93] Roddier, C. og Roddier, F. : **Wave–front reconstruction from defocused images and the testing of ground–based optical telescopes** , J. Opt. Soc. Am. A., Vol 10, No 11/November 1993/p. 2277-

[Sarazin, M. 89] Sarazin, M. and Roddier, F. : **The ESO differential image motion monitor**, ASTRON. AND ASTROPHYS., **227**, 294.

[Vernin, J. 95] Vernin, J. and Muñoz-Tuñó, C. : **Measuring Astronomical Seeing: The DA/IAC DIMM.**, PASP 107:265-272, March 1995

[Voitsekhovich, V. 95] Voitsekhovich, V. V. and Cuevas, S.: **Adaptive optics and the outer scale of turbulence**, J. Opt. Soc. Am., Vol 12, No 11/November 1995/p. 2523 - 2532